Indian Journal of Geo Marine Sciences
Vol. 49 (02), February 2020, pp. 201-206

# Remote sensing and airborne geophysics studies for uranium and thorium exploration in Zahedan area (Southeastern Iran)

Mehdi Hashemi

Department of Geology, Payame Noor University, PO Box 19395-3697, Tehran, Iran

**[**E-mail: economic.geology@yahoo.com**]**

*Received 27 July 2018; revised 05 May 2018*

The study area is located in Nehbandan-Khash zone according to the structural classification of Iran. The outcrops of this area are mainly composed of Cenozoic and Quaternary units. The structure of the area, under the influence of faults and folding, has a trend from north-northwest to south-southeast. Airborne data of radiometric was collected in the study area. In the exploration area of Zahedan, after processing and statistical analysis airborne radiometric data and preparing the map of the radioactive elements with the same intensity, the anomaly ranges were determined. For this purpose, two Ordinary Kriging and inverse distance squared technique were used to estimate the data. The trend of these radioactive element anomalies in the area was the general northwest-southeast trend, as identified in the maps. These anomalies of the radioactive elements are found in the Oligo-Miocene granodiorites units. Three anomaly ranges are located in the north-eastern corner of the sheet, which are proposed as valuable anomalies for continuing exploratory study.

**[Keywords**: Anomalies; Granodiorite; Radiometry; Radioactive elements; Zahedan]

## Introduction

In terms of frequency, Uranium is in the 48$^{th}$ place among the natural elements of the Earth's crust. Uranium is naturally found in the form of oxides or salts mixed in minerals (such as Uraninite or Carnotite). Uranium is one of the densest radioactive metals found in nature. The pure uranium is about 7.18 times denser than water and, like many other radioactive materials, is found as isotopes in nature. Uranium has sixteen isotopes. Natural uranium contains 3.99 % of the isotope $U^{238}$ and 7.0 % of the isotope $U^{235}$. Other isotopes of uranium are very rare. The isotope 235 is much more important than the isotope 238 in obtaining energy, as it can be easily split under certain conditions, yielding a lot of energy[1].

Thorium is a weekly radioactive metallic chemical element with the symbol Th and atomic number 90. Thorium is a naturally occurring, slightly radioactive element. It is found in small amounts in most rocks, where it is about three times abundant than uranium. Thorium is relatively enriched in acid igneous rocks, especially in granites. The most common thorium mineral is monazite. In uranium ore deposits, thorium is concentrated in thorite and thorianite[2].

Airborne geophysics produces additional data supplementing other available information (geological maps, etc.) to support better descriptions and a better understanding of the subsurface[3-5]. Airborne radioactivity studies are applied for minerals other than uranium and thorium, such as heavy minerals containing titanium and zirconium, tantalum, niobium, and rare-earth minerals. In this regard, carbonatites have a very low uranium-thorium ratio[6].

The present study firstly aims to process and analyse the airborne radiometric data of the study area.

## Materials and Methods

### Geographic location and access routes

The study area is located in the south-eastern part of Iran, in Sistan and Baluchistan Province (Fig. 1), in the Zahedan 1: 250000 and 1: 100000 geological sheets[7,8]. The area is located in Nehbandan-Khash zone according to the structural classification of Iran[9].

It has an arid and warm climate, and precipitation amount is also negligible in this area.

### Research method and sampling method

Radioactive radiation can be measured using the Geiger Müller counter, whose name was derived from its inventors. When radioactive radiation enters this counter, the gas contained in it carries electricity. The amount of charge can be read on the screen, or can be heard as a ticking tone through a speaker (Fig. 2).


Fig. 1— Location of the study area.

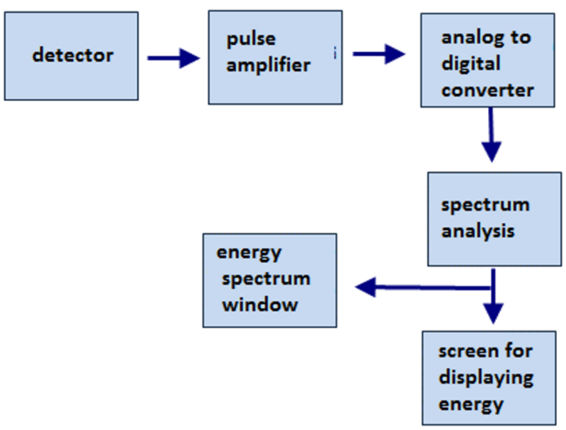


Fig. 2 — General view of the gamma ray spectrometer.

Airborne radiometric data was collected from the study area. Later on the airborne geophysical data were corrected, and then, different analyses were performed on the data. During geophysical data analysis, the anomaly-background separation was carried out using the classic statistical method. Two Ordinary Kriging and inverse distance squared technique were used to estimate data. Then, the radioactive elements map was processed and the results were interpreted to determine the range of uranium anomalies. Suitable areas for the study of radioactive elements were introduced. Those areas indicating the presence of radioactive elements were introduced method. Two Ordinary Kriging and inverse distance squared techniques were used to estimate data. Then, the radioactive elements map was processed and the results were interpreted to determine the range of uranium anomalies. Suitable areas for the study of radioactive elements were introduced indicating the presence of radioactive elements.

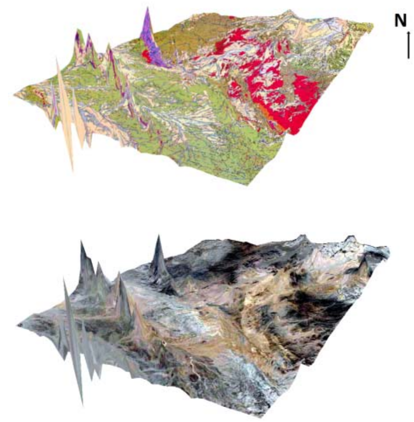


Fig. 3 — Adaptation on the geological map and aerial photo of the study area.

**Geology**

The outcrops of this area are mainly composed of Cenozoic and Quaternary rocks (Fig. 3).

**Cenozoic units**

Cenozoic units of the case study are divided into 4 categories:

1. Sedimentary units such as mudstone, siltstone with the interlayers of lime as well as conglomerate which are abundantly found in the area, especially in southern parts of the area.

2. Volcanic, andesitic volcanic and mafic basalt that are seen as narrow strips in the southwestern part of the area.

3. Metamorphic rocks and schists that cover the northern part of the area.

4. Intrusive rocks of the area that are categorized into two main and secondary categories:

A. Main intrusive rocks: These masses mainly include granodiorites, with which various types of acid and intermediate masses can be observed. These masses are found in the center of the range, with the northwest-southeast trend, as a wide strip.

B. Secondary intrusive rocks: A group of these masses are of diorite, granodiorite, tonalite, and quartz monzonite and can be observed in the western part of the area. The other group includes intermediate dikes, with which there are different types of mafic dikes. These dikes are widely spread in all parts of the area, especially in the northern part.

Table 1 — Statistical parameters of radioactive data of Uranium in Zahedan sheet

| | X | Y | U(eppm) |
|---|---|---|---|
| Mínimum: | 255658.5 | 3210215 | 0.62 |
| 25 %-tile: | 267658.5 | 3224215 | 1.512 |
| Median: | 279658.5 | 3238215 | 1.688 |
| 75 %-tile: | 291658.5 | 3253215 | 1.876 |
| Maximum: | 303658.5 | 3267215 | 3.228 |
| Midrange: | 279658.5 | 3238715 | 1.924 |
| Range: | 48000 | 57000 | 2.608 |
| Interquartile Range: | 24000 | 29000 | 0.364 |
| Median Abs. Deviation: | 12000 | 14000 | 0.181 |
| Mean: | 279626.9732554 | 3238598.9886645 | 1.6965154091392 |
| Trim Mean (10 %): | 279626.6227863 | 3238588.4750098 | 1.6948351042897 |
| Standard Deviation: | 14153.805636619 | 16728.455315622 | 0.29821113910374 |
| Variance: | 200330213.99919 | 279841217.24677 | 0.088929883485548 |
| Coef. of Variation: | | | 0.17577862098821 |
| Coef. of Skewness: | | | 0.16788579118055 |

**Quaternary units**

These units include alluvium, channel fill and old and young fan sediments. Quaternary travertine deposits can also be observed almost in the central part of the area.

## Discussion

To analyse the data statistically, SPSS and Excel software were used. Firstly, aerial radiometric information including survey points coordinates (UTM) was prepared in a file with Excel format and then, statistically processed by SPSS software.

In order to better understand the situation of the radioactive elements of the area, statistical doings were first performed on airborne geophysical data. For this, the data were first sorted, and then the data of uranium, thorium and potassium elements were filtered and classified. After these stages, frequency distribution tables and frequency distribution histograms were plotted, followed by calculation of the statistical parameters of these elements. Then, the anomaly separation was performed based on dispersion around the mean. The most important statistical parameters used in the interpretation of data and the anomaly-background separation, are mean, median, mode, diffraction, standard deviation, coefficient of variation, skewness and kurtosis.

These parameters were calculated for uranium and thorium elements using the aerial radiometric data of area.

Table 1 shows the results of the processes, such as minimum and maximum values, mean, and standard deviations. Table 2 shows statistical parameters of existing data. Figure 4 also shows the distribution of these data. It can be seen that, these data have an almost normal distribution.

| Gridding Rules | |
|---|---|
| Gridding Method | Inverse Distance to a Power |
| Weighting Power | 2 |
| Smoothing Factor | 0 |
| Anisotropy Ratio | 1 |
| Anisotropy Angle | 0 |
| **Search Parameters** | |
| Search Ellipse Radius #1 | 37300 |
| Search Ellipse Radius #2 | 37300 |
| Search Ellipse Angle | 0 |
| Number of Search Sectors | 4 |
| Maximum Data Per Sector | 16 |
| Maximum Empty Sectors | 3 |
| Minimum Data | 8 |
| Maximum Data | 64 |

Table 2 — Statistical parameters of existing data

| Statistics Table | | |
|---|---|---|
| N | Valid | 2838 |
| | Missing | 0 |
| Mean | | -179.541 |
| Median | | -190.4 |
| Std. Deviation | | 37.069 |
| Variance | | 1374.113 |
| Skewness | | 0.871 |
| Kurtosis | | 2.922 |
| Minimum | | -457.8 |
| Maximum | | 60.6 |
| Sum | | -509538 |
| Percentiles | 25 | -201 |
| | 50 | -190.4 |
| | 75 | -160.8 |

After statistical analysis and preparation of the maps of points with the same grade, the data were

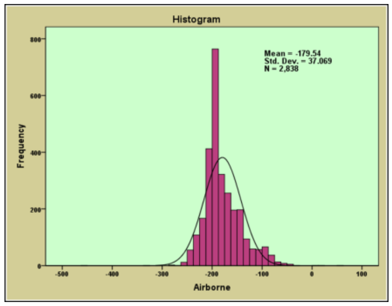


Fig. 4 — Histogram of collected data frequency.

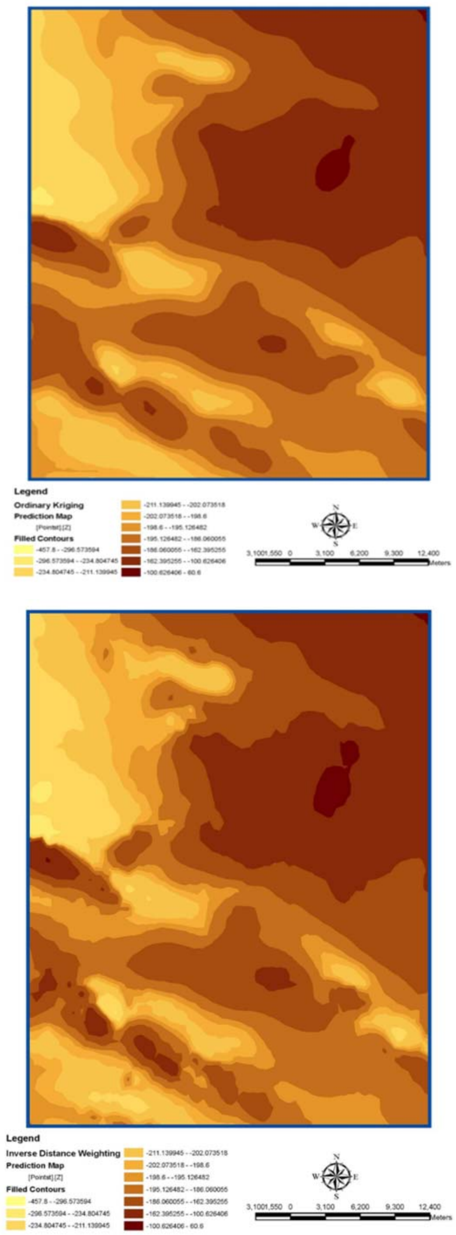

Fig. 5 — Estimation of airborne data of Zahedan area using: (a) Ordinary Kriging technique (b) Inverse-distance Squared technique.

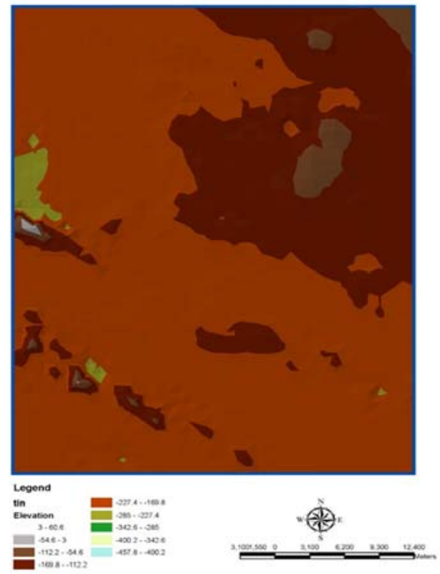

Fig. 6 — The map of the points with the same values based on airborne data of Zahedan area.

introduced to the ArcGIS software. Then, the data were classified and the possible anomalies were displayed in the best form. For this purpose, the data were classified into 10 classes, and then, they were estimated using two Ordinary Kriging and inverse-distance squared techniques[10,11] (Fig. 5a - b, 6).

Among the available data, the only data with a value of -457.8 had a different identity but removal of it was avoided in order to demonstrate its impact on the existing community.

Figure 7a shows the map of uranium dispersion in the Zahedan area. There is the map of dispersion of radioactive data of uranium with network estimation using inverse distance squared technique (Fig. 7b) and using Ordinary Kriging Technique (Fig. 8) in Zahedan exploration area. Figure 9 shows the map of dispersion of radioactive data of thorium in the Zahedan exploration area.

Table 3 shows statistical parameters of radioactive data of Uranium and Kriging network estimation and Table 4 shows statistical parameters of radioactive data of Thorium in Zahedan sheet.

Based on maps of dispersion of radioactive data of uranium obtained from two Ordinary Kriging and inverse distance squared technique, the radioactive element anomalies in the area were general northwest-southeast trend. These anomalies are found in the Oligo-Miocene granodiorites units. Three anomalies were located in the north-eastern corner of the sheet, which are proposed as significant anomalies.

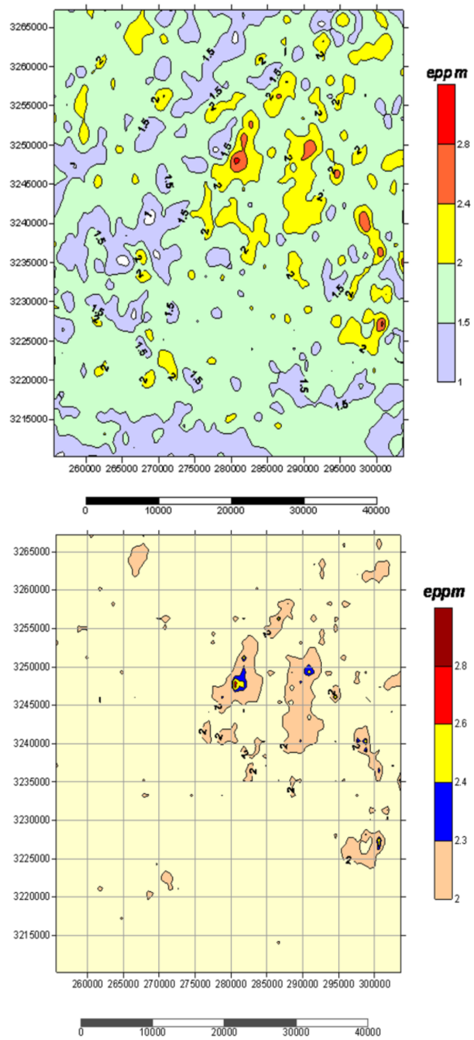


Fig. 7 — The map of dispersion from radioactive data of ((a) uranium, and (b) Uranium with network estimation using inverse distance squared technique) in Zahedan exploration area.

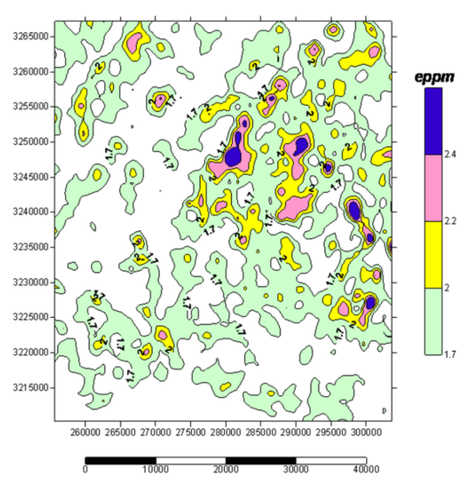


Fig. 8 — The map of dispersion of radioactive data of uranium with network estimation using Ordinary Kriging technique in Zahedan exploration area.

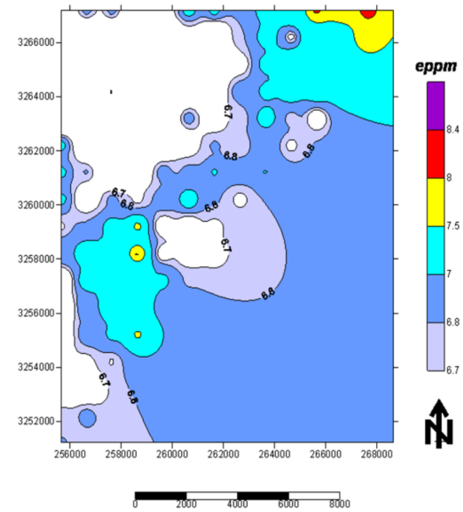


Fig. 9 — The map of dispersion of radioactive data of thorium in Zahedan exploration area.

Table 3 — Statistical parameters of radioactive data of uranium and Kriging network estimation in Zahedan sheet

| | X | Y | U(eppm) |
|---|---|---|---|
| Minimum: | 255658.5 | 3210215 | 0.62 |
| 25%-tile: | 267658.5 | 3224215 | 1.512 |
| Median: | 279658.5 | 3238215 | 1.688 |
| 75%-tile: | 291658.5 | 3253215 | 1.876 |
| Maximum: | 303658.5 | 3267215 | 3.228 |
| Midrange: | 279658.5 | 3238715 | 1.924 |
| Range: | 48000 | 57000 | 2.608 |
| Interquartile Range: | 24000 | 29000 | 0.364 |
| Median Abs. Deviation: | 12000 | 14000 | 0.181 |
| Mean: | 279626.9732554 | 3238598.9886645 | 1.6965154091392 |
| Trim Mean (10%): | 279626.6227863 | 3238588.4750098 | 1.6948351042897 |
| Standard Deviation: | 14153.805636619 | 16728.455315622 | 0.29821113910374 |
| Variance: | 200330213.99919 | 279841217.24677 | 0.088929883485548 |
| Coef. of Variation: | | | 0.17577862098821 |
| Coef. of Skewness: | | | 0.16788579118055 |

Grid Statistics

| | |
|---|---|
| Z Minimum: | 0.771508742 |
| Z 25%-tile: | 1.535182863 |
| Z Median: | 1.692821146 |
| Z 75%-tile: | 1.860756669 |
| Z Maximum: | 2.900363529 |
| Z Midrange: | 1.835936135 |
| Z Range: | 2.128854787 |
| Z Interquartile Range: | 0.325573806 |
| Z Median Abs. Deviation: | 0.162556769 |
| Z Mean: | 1.698582569 |
| Z Trim Mean (10 %): | 1.69713183 |
| Z Standard Deviation: | 0.261893905 |
| Z Variance: | 0.068588417 |
| Z Coef. of Variation: | 0.154183794 |
| Z Coef. of Skewness: | 0.129674184 |
| Z Root Mean Square: | 1.71865388 |
| Z Mean Square: | 2.95377116 |

Table 4 — Statistical parameters of radioactive data of Thorium in Zahedan exploration area

| | X | Y | Th(eppm) |
|---|---|---|---|
| Minimum: | 255643.5 | 3251215 | 5.7 |
| 25 %-tile: | 256643.5 | 3259215 | 6.386 |
| Median: | 259643.5 | 3262215 | 6.78 |
| 75 %-tile: | 262643.5 | 3265215 | 7.139 |
| Maximum: | 268643.5 | 3267215 | 8.372 |
| Midrange: | 262143.5 | 3259215 | 7.036 |
| Range: | 13000 | 16000 | 2.672 |
| Interquartile Range: | 6000 | 6000 | 0.753 |
| Median Abs. Deviation: | 3000 | 3000 | 0.378 |
| Mean: | 259953.02380952 | 3261881.6666667 | 6.7872619047619 |
| Trim Mean (10 %): | 259792.62280702 | 3262083.4210526 | 6.7666228070175 |
| Standard Deviation: | 3384.0529042787 | 4109.6093353126 | 0.49982308264583 |
| Variance: | 11451814.058957 | 16888888.888889 | 0.24982311394558 |
| Coef. of Variation: | | | 0.073641343101134 |
| Coef. of Skewness: | | | 0.5385746797401 |

Grid Statistics

| | |
|---|---|
| Z Minimum: | 5.712994158 |
| Z 25 %-tile: | 6.729384401 |
| Z Median: | 6.818683386 |
| Z 75 %-tile: | 6.87739059 |
| Z Maximum: | 8.368421604 |
| Z Midrange: | 7.040707881 |
| Z Range: | 2.655427447 |
| Z Interquartile Range: | 0.148006189 |
| Z Median Abs. Deviation: | 0.070898664 |
| Z Mean: | 6.81296191 |
| Z Trim Mean (10 %): | 6.804595775 |
| Z Standard Deviation: | 0.249581867 |
| Z Variance: | 0.062291108 |
| Z Coef. of Variation: | 0.036633387 |
| Z Coef. of Skewness: | 0.716011266 |
| Z Root Mean Square: | 6.817531892 |
| Z Mean Square: | 46.4787411 |

## Conclusion

In the Zahedan exploration area, after processing and analysing the airborne radiometric data and preparing the maps of the radioactive elements with the same intensity, area anomalies was determined. The anomalies of these radioactive elements had northwest-southeast trend, as shown in the maps prepared. These anomalies of the radioactive elements are found in the Oligo-Miocene granodiorites units. Three anomaly ranges are located in the north-eastern corner of the sheet, which are proposed as valuable anomalies for continuing exploratory study.

## Acknowledgment

We thank to the Atomic Energy Organization of Iran who helped us in carrying out the present research.

## Reference

1 Chen, Z., Regional distribution of uranium deposits in Northern Asian, sandstone-type Uranium Deposits in China. *Geo. Explor. Tech*, (2012): 24-32.
2 Rene, M., Nature, Sources, Resources, and Production of Thorium, Descriptive Inorganic Chemistry Researches of Metal Compounds, Takashiro Akitsu, Intech Open, DOI: 10.5772/Intech open.(2017): 68304.
3 Ranjbar, H., Hassanzadeh, H., Torabi, M., & Ilaghi, O., Integration and analysis of airborne geophysical data of the Darrehzar area, Kerman Province, Iran, using principal component analysis. *J. Applied geophysics,* 48 (2001): 33-41.
4 Ranjbar, H., & Honarmand, M., Integration and analysis of airborne geophysical and ETM+ data for exploration of porphyry type deposits in the central Iranian volcanic belt using fuzzy classification, *Int. J. Remote Sens.,* 25 (21) (2004): 4729-4741.
5 Honarmand, M., Integration of Aster and airborne geophysical data of copper mineralization. A case study of Sarcheshmeh area, *International society for photogrammetry and remote sensing*, Turkey, (2004), 12-23.
6 Gunn, P.J., Fitzgerald, D., Yassi, N., & Dart, P., New algorithm for visually enhancing airborne geophysical data. *Explor. Geophysic*, 28 (2010): 220-224.
7 Berberian, M., Geological map of the Zahedan area, scale 1:100,000. *Geol. Surv. Iran*, (1983), sheet 8148.
8 Saidi, A., Geological map of the Zahedan area, scale 1:25 0,000. *Geol. Surv. Iran*, (1995), sheet 9311.
9 Aghanabati, A., Geology of Iran, *Geological Survey of Iran*, Tehran, Iran, (2005), p. 619.
10 Zia Zarifi, A., *The basics of geophysical radiometric exploration*. Lahijan Islamic Azad University Press, (2017): 308.
11 Hasani Pak, A.A., & Sharaf al-Din, M., *Exploratory data analysis*. University Tehran Press. (2015).